0013-7227/04/$15.00/0
Printed in U.S.A.

Endocrinology 145(7):3386–3394

doi: 10.1210/en.2003-1710

Rhythmic Secretion of Prolactin in Rats: Action of Oxytocin Coordinated by Vasoactive Intestinal Polypeptide of Suprachiasmatic Nucleus Origin

MARCEL EGLI, RICHARD BERTRAM, MICHAEL T. SELLIX, AND MARC E. FREEMAN

Departments of Biological Science (M.E., M.T.S., M.E.F.) and Mathematics and Kasha Laboratory of Biophysics (R.B.), Florida State University, Tallahassee, Florida 32306

Prolactin (PRL) is secreted from lactotrophs of the anterior pituitary gland of rats in a unique pattern in response to uterine cervical stimulation (CS) during mating. Surges of PRL secretion occur in response to relief from hypothalamic dopaminergic inhibition and stimulation by hypothalamic releasing neurohormones. In this study, we characterized the role of oxytocin (OT) in this system and the involvement of vasoactive intestinal polypeptide (VIP) from the suprachiasmatic nucleus (SCN) in controlling OT and PRL secretion of CS rats. The effect of OT on PRL secretion was demonstrated in cultured lactotrophs showing simultaneous enhanced secretion rate and increased intracellular Ca^{2+}. Neurosecretory OT cells of the hypothalamic paraventricular nucleus that express VIP receptors were identified by using immunocytochemical techniques in combination with the retrogradely transported neuronal tracer Fluoro-Gold (iv injected). OT measurements of serial blood samples obtained from ovariectomized (OVX) CS rats displayed a prominent increase at the time of the afternoon PRL peak. The injection of VIP antisense oligonucleotides into the SCN abolished the afternoon increase of OT and PRL in CS-OVX animals. These findings suggest that VIP from the SCN contributes to the regulation of OT and PRL secretion in CS rats. We propose that in CS rats the regulatory mechanism(s) for PRL secretion comprise coordinated action of neuroendocrine dopaminergic and OT cells, both governed by the daily rhythm of VIP-ergic output from the SCN. This hypothesis is illustrated with a mathematical model. (*Endocrinology* 145: 3386–3394, 2004)

PROLACTIN (PRL) is one of the most versatile hormones of mammalian organisms. It plays a key role in lactation and contributes to a wide range of physiological functions (1). In the rat, PRL is secreted in various patterns depending on the physiological state of the animal. Pronounced PRL release is initiated in cycling rats during the afternoon of proestrus every fourth or fifth day or by nursing pups on lactating dams. Stimulation of the uterine cervix (CS) during mating (leading to pregnancy/pseudopregnancy) induces a PRL secretory pattern consisting of nocturnal surges (N) between 0100 and 0500 h, and diurnal surges (D) between 1600 and 1800 h (1).

PRL is synthesized and secreted by lactotrophs in the anterior lobe of the pituitary gland (1). Its release is under tonic inhibition by dopamine (DA) (2), originating from three distinct hypothalamic neuronal populations (3). It has been shown that coincident with the release of PRL, DA levels in the portal blood that supplies the anterior lobe is reduced (4, 5). However, the temporary reduction of the PRL-inhibiting hormone (PIH) DA does not fully account for the entire amount of PRL released. Additional PRL-releasing neurohormones (PRH) of hypothalamic origin may be involved in the formation of the surges (1). Oxytocin (OT) is one promising PRH candidate. Several *in vivo* and *in vitro* studies have indicated a stimulatory effect of OT on the release of PRL (1, 6, 7). The infusion of OT antagonist also suppressed both the N and D PRL surges of CS rats (8). Furthermore, *in situ* hybridization studies have shown OT receptor mRNA expression in lactotrophs (9).

Neurons in the paraventricular nucleus (PVN) of the hypothalamus are major production sites for OT (10). It has been shown that OT neurons in PVN of OVX rats display daily activity rhythms that correlate with the PRL-releasing pattern in CS rats (11).

The suprachiasmatic nucleus (SCN) of the hypothalamus is known for its pacemaker function, responsible for timing circadian rhythms in mammals (12). The nucleus can be subdivided into a shell and core region; the core dominated by vasoactive intestinal polypeptide (VIP)-producing neurons (13). Neuronal tract-tracing studies demonstrated efferent connections from SCN to PVN in rats (14). Further studies identify these efferents as VIPergic, innervating several regions of the hypothalamus (15) and *in situ* hybridization studies have verified VIP2 receptor mRNA expression within the PVN (16). Immunocytochemical investigations and mRNA measurements in the SCN revealed a daily rhythm of VIP that peaks during the dark phase (17–19). This rhythm is absent under constant dark conditions (19) and is reduced in unilaterally enucleated rats (20).

We hypothesize that OT acts as a PRH in CS rats. In our model, the SCN serves as a pacemaker, dictating the activity pattern of hypothalamic DA and OT neurons via its rhythmic

Abbreviations: aCSF, Artificial cerebrospinal fluid; AS, antisense; CS, cervical stimulation; D, diurnal surges; DA, dopamine; FG, FluoroGold; HBS, HEPES-buffered saline; ICC, immunocytochemistry; N, nocturnal surges; ODN, oligodeoxynucleotide; OT, oxytocin; OVX, ovariectomized; PeVN, periventricular nucleus; PIH, PRL-inhibiting hormone; PRH, PRL-releasing neurohormones; PRL, prolactin; PVN, paraventricular nucleus; RS, random sequence; SCN, suprachiasmatic nucleus; VIP, vasoactive intestinal peptide.

***Endocrinology* is published monthly by The Endocrine Society (http://www.endo-society.org), the foremost professional society serving the endocrine community.**

VIP output. We illustrate this hypothesis with a mathematical model that demonstrates how VIPergic control of DA and OT neurons may produce the characteristic PRL secretory pattern in CS rats.

Materials and Methods

Animals

Adult female Sprague Dawley rats (Charles River, Raleigh, NC; 200–250 g) were kept in standard rat cages under a 12-h light, 12-h dark cycle (lights on at 0600 h) with water and rat chow *ad libitum*. All animals were bilaterally ovariectomized (OVX) under Halothane anesthesia. The uterine cervix was electrically stimulated with two platinum electrodes placed 2 mm apart at the tip of a Teflon rod. The first CS was applied 30 h (at 1700 h) and the second 15 h (at 0900 h) before the first blood sampling time. Stimulations were applied as two consecutive trains of electric current of 10-sec duration (rectangular pulses 1 msec of 40 V at 200 Hz). This procedure has been shown to yield the highest success rate in initiating two daily PRL surges characteristic of pregnant/pseudopregnant rats (21). All animal procedures were approved by the Florida State University Animal Care and Use Committee.

SCN guide cannula and jugular vein catheter implantation

Rats were anesthetized with a mixture of Ketamine (65 mg/kg) and Xylazine (4 mg/kg) and placed in a stereotaxic frame. After drilling a hole through the skull, bilateral stainless steel guide cannulae (26 gauge, 1 mm apart; Plastics One, Roanoke VA) were lowered to the dorsal border of the SCN (coordinates according to the rat atlas by Paxinos and Watson (22): 0.7 mm caudal to Bregma and 7.9 mm ventral to the dura mater). The cannulae were held in place by dental cement anchored by screws.

Polyurethane catheter tubing (Micro-Renathane, Braintree Scientific Inc., Braintree, MA), extended with Tygon tubing (TGY-040-100, Small Parts Inc., Miami Lakes, FL), was inserted into the jugular vein while the rats were anesthetized with Halothane. The tubing, filled with heparinized saline (50 U/ml), was fitted sc and exteriorized at the back of the animal's neck. A daily flush with heparinized saline kept the line open until the start of the blood collection at 2300 h, 5 d after surgery.

RIA

Serum concentrations of PRL were estimated in duplicate by the rat PRL RIA kit as previously described (23). Rat PRL RP-3 standard was supplied by Dr. Albert Parlow through the National Hormone and Pituitary Program (Torrance, CA). The measurement of serum OT concentration was performed with the Phoenix OT kit (Phoenix Pharmaceuticals Inc., Belmont, CA, validated for the use of rat serum) according to the manufacturer's protocol. The assay sensitivity was 1 pg/ml serum.

VIP antisense (AS) oligonucleotide injections

Phosphorothioated oligodeoxynucleotides (ODNs) dissolved in artificial cerebrospinal fluid (aCSF) were infused through 33-gauge needles inserted in the guide cannulae. The AS-ODNs were 20 oligomers complementary to the cap site (5′-GCTCTGCACTACAACCTGAC-3′) and translation start site (5′-TTGCTTCTGGATTCCATCTC-3′) of the rat VIP mRNA. Control random sequence (RS)-ODNs were 20 oligomers with the same ATGC content as the AS-oligos but in RS that had no significant homology to any known peptides localized in the SCN (24). Each side of the SCN received a 0.4-μl injection (applied within 1 min) of the corresponding ODN (ODN: 1 μg/μl in 0.9% saline solution; aCSF: 125 mM NaCl, 2.5 mM KCl, 1.25 mM NaH_2PO_4, 1 mM $MgCl_2$, 25 mM $NaHCO_3$, 2 mM $CaCl_2$, 25 mM glucose), 36 h before the first blood collection time point. This dose has been previously reported not to result in significant side effects or toxicity when used for SCN injection (24). ODN were produced locally at the Florida State University Biochemical Analysis and Synthesis Service laboratory.

Blood collection

Starting at 2300 h 5 d after surgery, 200 μl of blood were collected at 2-h intervals over a period of 24 h (excluding the 0900 h time point). Serum samples were stored at 4 C until analysis.

Immunocytochemistry (ICC)

Rats were transcardially perfused with 60 ml of cold perfusion rinse (0.5% $NaNO_2$ in 0.9% saline solution) followed by 300 ml of cold 4% paraformaldehyde in 0.1 M PBS (pH 7.2). The brains were removed, postfixed in 4% paraformaldehyde/PBS overnight, and placed in 20% sucrose/PBS for at least 12 h. Coronal sections (40 μm) of the brains (through SCN and PVN) were cut on a freezing microtome and stored in cryoprotectant (25). Before the incubation with the primary antibody (for 24 h at 4 C), the sections were washed three times in 0.1% Triton X-100 in PBS and exposed to 10% normal goat serum (Chemicon, Temecula, CA) in PBS for 1 h. Depending on the experiment, the following primary antibody combinations were used: 1) OT (rabbit anti-OT, IHC8152, Peninsula Laboratories, Inc., Belmont, CA; dilution 1:5000); 2) OT and VIP receptor subtype 2 (mouse anti-VIP2R, AS69-P, Antibody Solutions, Palo Alto, CA; dilution 1:600) together or 3) VIP (sheep anti-VIP, AB 1581, Chemicon International Inc.; dilution 1:5000). The binding specificity of the antibodies were published in a previous study (26). To test for specificity of label in our ICC protocol, tissue sections were incubated in antibody against VIP2R that had been preabsorbed with the immunizing VIP2R peptide (corresponding to amino acids 105–122; Antibody Solutions), whereas other sections were incubated in buffer without primary antibody. Secondary antibodies, conjugated to fluorescent probes CY2 (donkey antirabbit/sheep, Jackson ImmunoResearch, West Grove, PA) or CY3 (donkey antigoat/mouse, Jackson ImmunoResearch), were added in the concentration of 1:600 for another 24 h at 4 C. All primary and secondary antibodies were diluted in 0.4% Triton X-100/0.01% Na-Azide in PBS. Finally, sections were mounted on glass slides, coverslips applied with Aqua Polymount (Polysciences, Inc., Warrington, PA), and sealed with nail polish.

For the quantification of protein expression levels after the VIP AS-ODN injection, three 40 μm-thick coronal brain sections through the ventrolateral SCN (13) were analyzed per animal for the intensity of VIP immunoreactivity as described by Turgeon *et al.* (27) and Gerhold *et al.* (24). Two images were taken by a digital camera (SPOT camera, Diagnostic Instruments Inc., Sterling Heights, MI) per brain section (right and left core region of SCN) on a fluorescent microscope (Leica, Wetzlar, Germany). Using the image analysis software MetaMorph (version 5.0r1, Universal Imaging Corp., Downingtown, PA), the mean pixel intensity of staining was calculated (relative intensity units) within a circle (d = 400 μm, Fig. 4A) encompassing the core region of SCN. The bases for the calculation were 8-bit monochrome images with a range of 255 gray values. At the end, one average number of mean ICC VIP staining intensity in the SCN was calculated per animal.

Fluoro-Gold (FG) and OT double labeling

The systemic administration of FG (Fluorochrome, LLC, Denver, CO) is a well-established method for labeling neurosecretory cells (28–30). In our experiments, the rats (n = 3) received an injection of 20 mg/kg body weight FG, dissolved in 0.9% saline, via the tail vein. After 72 h, the same procedure as described above was used for fixing, cutting, and ICC OT labeling.

Dispersion of AP glands and lactotroph enrichment

The dispersion of AP glands was similar to our previous published protocol (31). Before plating, the cell suspension was enriched for lactotrophs using a slightly modified version of the Percoll discontinuous density gradient enrichment protocol (32), yielding 75–90% lactotrophs. Briefly, the suspension was applied on top of a Percoll (Sigma, St. Louis, MO) density gradient [50% and 35% Percoll in HEPES-buffered saline (HBS)]. After 20 min of centrifugation (700 G), the interface was gently aspirated and transferred into HBS. After rinses in HBS and centrifugation (two times), cells were plated on 35-mm poly-L-lysine (Sigma)-coated glass coverslips in a density of 10^6 cells/coverslip and stored in 10% fetal bovine serum (FBS, Intergen, Purchase, NY)/DMEM (Invitrogen Life Technologies, Rockville, MD). The cultures were kept in a CO_2 incubator at 5% CO_2 and 37 C for 2 d before use in Ca^{2+} imaging studies. Lactotrophs express TRH receptors (33) and release PRL in response to TRH in a dose-dependent manner (1). Furthermore, the calcium-mobilizing actions of TRH on lactotrophs have been well characterized (34). Therefore, lactotrophs were further identified by their *post hoc* response to TRH application as well as their cell type-specific morphology.

Intracellular Ca^{2+} recordings

Intracellular Ca^{2+} ($[Ca^{2+}]_i$) was determined by quantitative fluorescent microscopy using the calcium probe Fura-2/AM (Molecular Probes, Eugene, OR) as described previously (35). In brief, after three HBS washes, the coverslips bearing cultured lactotrophs were incubated with 5 μM Fura-2/AM in HBS for 30 min at 37 C in a CO_2 incubator before placement in a Dvorak-Stotler chamber. Average intensities of light emission of each cell were measured at 510 nm by a digital camera (C4745-95, Hamamatsu Corp., Bridgewater, NJ) during exposure to alternating 340 nm and 380 nm light beams on an inverted microscope (Axiovert 35, Zeiss, Heidelberg, Germany). Intracellular Ca^{2+} is expressed as the ratio of 340 nm/380 nm of single cells that was calculated with the software MetaFluor (version 4.6r9, Universal Imaging Corp.). Lactotrophs were perfused with prewarmed HBS supplemented with $CaCl_2$ (2 mM) and $MgCl_2$ (1 mM) at a rate of 1 ml/min. Temperature was held constant at 37 C by an in-line solution heater (SH-27A, Warner Instruments, Inc., Hamden, CT). After establishing basal condition, test substances were applied for 2 min by switching to a perfusion solution containing OT (10^{-8}–10^{-6} M, Peninsula Laboratories, Inc.) or TRH (10^{-6} M). The effluent media were collected every minute by a fraction collector (FC 203, Gilson Inc., Middleton, WI) and stored at 4 C until PRL concentration was determined.

Data analysis and statistics

Fluorecent labeling in brain sections was visualized using the CY2-CY3 filter combination on a fluorescent microscope (Leica) and images produced with a digital camera (SPOT camera, Diagnostic Instruments Inc.). High resolution images of OT and VIP2R immunostained brain sections were taken with a confocal laser-scanning microscope (Zeiss LSM 510), equipped with Argon/2 (488 nm) and HeNe1 (543 nm) laser light sources. Images were acquired as a Z-series stack at 0.3 μm steps by using a ×40 Plan Neofluar 1.3NA oil objective lens in multitracking configuration. Depending on the region of interest, stacks of 20–60 optical sections (thickness of 0.9 μm) were taken from the specimens. Statistical analysis was performed using Microsoft Excel or GraphPad Prism 3.0 (GraphPad Software Inc., San Diego, CA). Significance was determined using one-way ANOVA and differences were considered significant if $P \leq 0.05$.

Modeling

Mathematical modeling was performed to help interpret the experimental data. The model consists of a set of three equations describing the time-dependent variation of PRL, DA, and OT concentrations. The equations reflect the stimulatory and inhibitory interactions among cell types, based on data reported in this study, as well as data from the literature. The first equation, for PRL, is

$$\frac{d\,\mathrm{PRL}}{dt} = r_\mathrm{P}\left[\frac{1}{k_\mathrm{D} + \mathrm{DA}}\right]\left[\frac{\mathrm{OT}}{k_\mathrm{O} + \mathrm{OT}}\right]^2 - q_\mathrm{P}\mathrm{PRL} \qquad (1)$$

The factor $1/(k_D + DA)$ is a decreasing function of DA concentration and reflects the inhibitory effect of DA on PRL secretion. The factor

$$\left[\frac{\mathrm{OT}}{k_\mathrm{O} + \mathrm{OT}}\right]^2$$

is an increasing sigmoidal function of OT concentration and reflects the stimulatory effect of OT. The final term, q_PPRL, accounts for removal of PRL from the system.

The second differential equation in the model describes the dynamics of DA,

$$\frac{d\,\mathrm{DA}}{dt} = q_\mathrm{D}(\mathrm{DA}_\infty - \mathrm{DA}) - \nu_\mathrm{D} \qquad (2)$$

The parameter DA_∞ is the steady-state or long-term value of the DA concentration. The term $q_\mathrm{D}(DA_\infty - DA)$ ensures that DA approaches its steady-state with a time constant of $1/q_\mathrm{D}$. The second term, ν_D, is set to a positive value during periods when there is inhibitory VIP input to DA neurons from the SCN (2 h at night in the simulation of VIP RS-ODN-treated animals). This causes DA concentration to decrease.

The third differential equation describes the dynamics of OT,

$$\frac{d\,\mathrm{OT}}{dt} = r_\mathrm{O}\left[\frac{x}{k_\mathrm{x} + x}\right] - q_\mathrm{O}\mathrm{OT} - \nu_\mathrm{O} \qquad (3)$$

The first term

$$r_\mathrm{O}\left[\frac{x}{k_\mathrm{x} + x}\right]$$

is an increasing function of the stimulatory factor x. The existence of such a factor is one of the predictions of the model. This is elevated twice per day in our simulations, at night and in the afternoon. The second term, q_OOT, reflects removal of OT from the system. The final term, ν_O, is a parameter that is elevated once per day (2 h at night in simulations of VIP RS-ODN animals) and reflects inhibitory VIP input onto OT cells.

Parameter values were adjusted to match the experimental PRL and OT time courses. Model equations were integrated using the CVODE numerical method as implemented in the program XPPAUT (36). Parameter values used in the integration are listed in Table 1. The model can be downloaded from our web site at www.neuro.fsu.edu/postDocs/egli or www.math.fsu.edu/~bertram.

Results

OT stimulates PRL secretion in lactotrophs through a calcium-dependent mechanism

To confirm that OT is a potent PRH, we investigated the response of lactotrophs to the application of OT by simultaneously monitoring fluctuations of $[Ca^{2+}]_i$ and PRL secretion in the perfusion media. For comparison, the PRL secretory response of lactotrophs to the application of TRH (10^{-6} M) 10 min after the OT challenge served as a reference (regarded as 100% response) (37).

Measurement of the concentration of PRL in effluent media from the recording chamber holding a coverslip with 10^6 cells, revealed a bell-shaped pattern (Fig. 1A) in response to varying concentrations of OT. In the absence of DAergic inhibition, unstimulated cells (C; Fig. 1A) secreted PRL at 35.4 ± 2.7% of the maximal TRH response (10^{-6} M) (mean ± SEM, n = 12 coverslips). The application of 10^{-8} M OT led to a significant ($P < 0.01$) increase in PRL secretion to 72.7 ± 8.8% (n = 4 coverslips) of the TRH response. Secretion peaked with the application of 10^{-7} M OT (91.7 ± 10.6%, $P < 0.01$, n = 3 coverslips). A higher dose of OT (10^{-6} M) yielded a smaller PRL secretory response (59.3 ± 7.6%, n = 5 coverslips) that was still significantly greater ($P < 0.05$) than the control value.

The $[Ca^{2+}]_i$ response to OT application (10^{-8}–10^{-6} M) was

TABLE 1. Parameter values used in the mathematical model (see *Materials and Methods* for parameter description)

Parameter	Value
DA_∞	20,000 ng/ml
k_D	300
k_O	9
k_x	50
q_D	0.2
q_O	1
q_P	0.5
r_O	1100
r_P	300,000
v_O	500
v_D	10,000

Initial values for DA, OT, and PRL were set to $DA(0) = 20{,}000$ ng/ml; $OT(0) = 25$ pg/ml; and $PRL(0) = 20$ ng/ml.

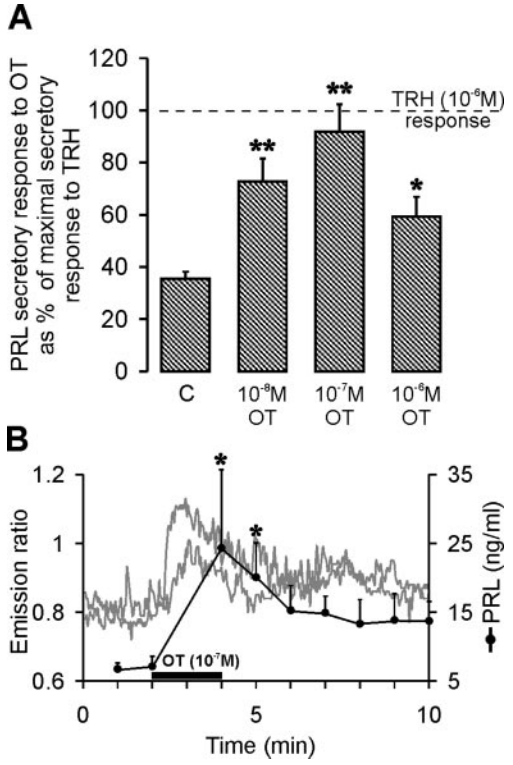

FIG. 1. OT-induced PRL secretion and $[Ca^{2+}]_i$ changes in cultured lactotrophs. A, Lactotrophs secreted PRL at a rate of 37.9 ± 3.1% of the maximal TRH response (n = 7 coverslips) in control conditions (C) and without DAergic inhibition. OT applied in various concentrations yielded secretion rates of 72.7 ± 8.8% (n = 4 coverslips) under 10^{-8} M and 91.7 ± 10.6%, (n = 3 coverslips) under 10^{-7} M. A higher OT concentration (10^{-6} M) reduced the PRL output to 59.3 ± 7.6% (n = 5 coverslips). Values represents the mean % of secretion rates ± SEM; significant differences from basal value are indicated: *, $P < 0.05$; **, $P < 0.01$. B, Application of 10^{-7} M OT for 2 min provoked a sudden and distinct increase of $[Ca^{2+}]_i$, expressed as an increase in the light emission ratios of Fura-2/AM-labeled cells (two representative cells). PRL secretion also increased, coincident with the $[Ca^{2+}]_i$ rise. Statistical tests revealed significant differences ($P < 0.05$) between basal PRL levels and the PRL levels 2 and 3 min after initiation of OT application. Values represent the mean ± SEM. PRL concentration (nanograms per milliliter) from three coverslips.

recorded from 340 individual cells, plated on 20 coverslips. Overall, 31% of these cells demonstrated an increase in the cytosolic Ca^{2+} concentration. Figure 1B displays the time course of the $[Ca^{2+}]_i$ response of two representative cells during and after OT (10^{-7} M) challenge. The application elicited a rapid rise in $[Ca^{2+}]_i$ to a peak within seconds followed by a return to a secondary elevated plateau level. The initial mean emissions ratio rose from 0.84 ± 0.05 up to 1.26 ± 0.13 ($P < 0.01$, n = 11 cells), under the 10^{-7} M OT treatment. Analysis of effluent media revealed that PRL secretion increased simultaneously with the $[Ca^{2+}]_i$ response in the presence of 10^{-7} M OT. The peak level of 24.3 ± 11.3 ng/ml secreted PRL was significantly ($P < 0.05$) higher than basal levels of 6.8 ± 0.9 ng/ml (n = 3 coverslips).

Neurosecretory OT neurons in the PVN and periventricular nucleus (PeVN) express VIP receptor

The retrogradely transported neurotracer FG (iv injected) in combination with ICC was used to identify neurosecretory OT cells. In addition, ICC was performed to determine the pattern of VIP2R expression in neurosecretory OT cells.

Anatomical analysis of OT-FG double staining showed colocalization of a majority of the OT neurons in the anterior magnocellular portion of the PVN (close to the ventral border of the fornix) and the PeVN (*yellow staining* in Fig. 2A). Similar strong OT-FG colocalization was found further caudal in the lateral and ventral portion of the PVN (*yellow staining* in Fig. 2B). The localization of OT neurons expressing VIP2R overlapped with OT-FG labeling, especially in the PeVN (*filled arrowheads* in Fig. 2C) and in the magnocellular portion of the PVN (*filled arrowheads* in Fig. 2D). Overlap in these two regions was more extensive than in the other portions of the PVN, where colocalization appeared in only a few scattered cells.

VIP AS oligonucleotide injection into SCN changes the pattern of PRL and OT secretion in CS rats

AS-ODN technique was used to determine the influence of VIP (of SCN origin) in the regulation of OT release and PRL secretion. The reduction of VIP expression caused by the injection of VIP AS-ODN was quantified by analysis of the mean pixel intensity of ICC VIP staining on SCN sections. In the same sections, proper cannula placement was verified (cannulae tip above the dorsal border of the SCN).

The experiments with ODN were performed using the same procedure as described previously (24). AS-ODN against VIP mRNA injected into the SCN caused an ablation of the D PRL surge and a shift of the afternoon OT surge. The remaining surges for both PRL (99.8 ± 34.2 ng/ml, mean ± SEM, n = 4; Fig. 3A, *open circles*) and OT (317.5 ± 128.5 pg/ml, n = 5; Fig. 3B, *open circles*) peaked simultaneously at 0300 h. Serum PRL measurements from CS-OVX rats, which received RS-ODN injection (as control) confirmed the well-known PRL secretory pattern of two peaks per day (N and D surges; Fig. 3A, *filled circles*). The serum concentration of PRL peaked at 0300 h (61.9 ± 37.6 ng/ml, n = 5) and at 1700 h (41.8 ± 8.5 ng/ml, n = 4). The concentration of OT in serum increased in the afternoon, with a peak value of 432.5 ± 161.4 pg/ml (n = 5) at 1300 h (Fig. 3B, *filled circles*). Additional control studies were performed on CS-OVX rats without SCN cannula. Blood serum analysis from these experiments demonstrated the same secretory pattern of PRL and OT to that of RS-ODN injected CS-OVX rats (data not shown).

The effect of VIP AS-ODN administration on VIP synthesis in the SCN is shown in Fig. 4. Compared with the control sections, the injection of the AS-ODN caused a significant reduction ($P < 0.05$) in VIP immunoreactivity (presented as pixel intensity). Figure 4A shows a photomicrograph of a representative SCN section of animals treated with VIP AS-ODN, 58 h after the ODN injection. The *dashed circles* in 4A demonstrate the position and the area used for the calculation of the mean pixel intensity, encompassing the core region of SCN on both sides of the third ventricle (III). In addition, the * in Fig. 4A indicates the placement of the former tip of the implanted bilateral cannulae. SCN brain sections of untreated animals (Fig. 4B) displayed a more intense VIP immunoreactivity.

Figure 4C shows a bar graph of the mean pixel intensity

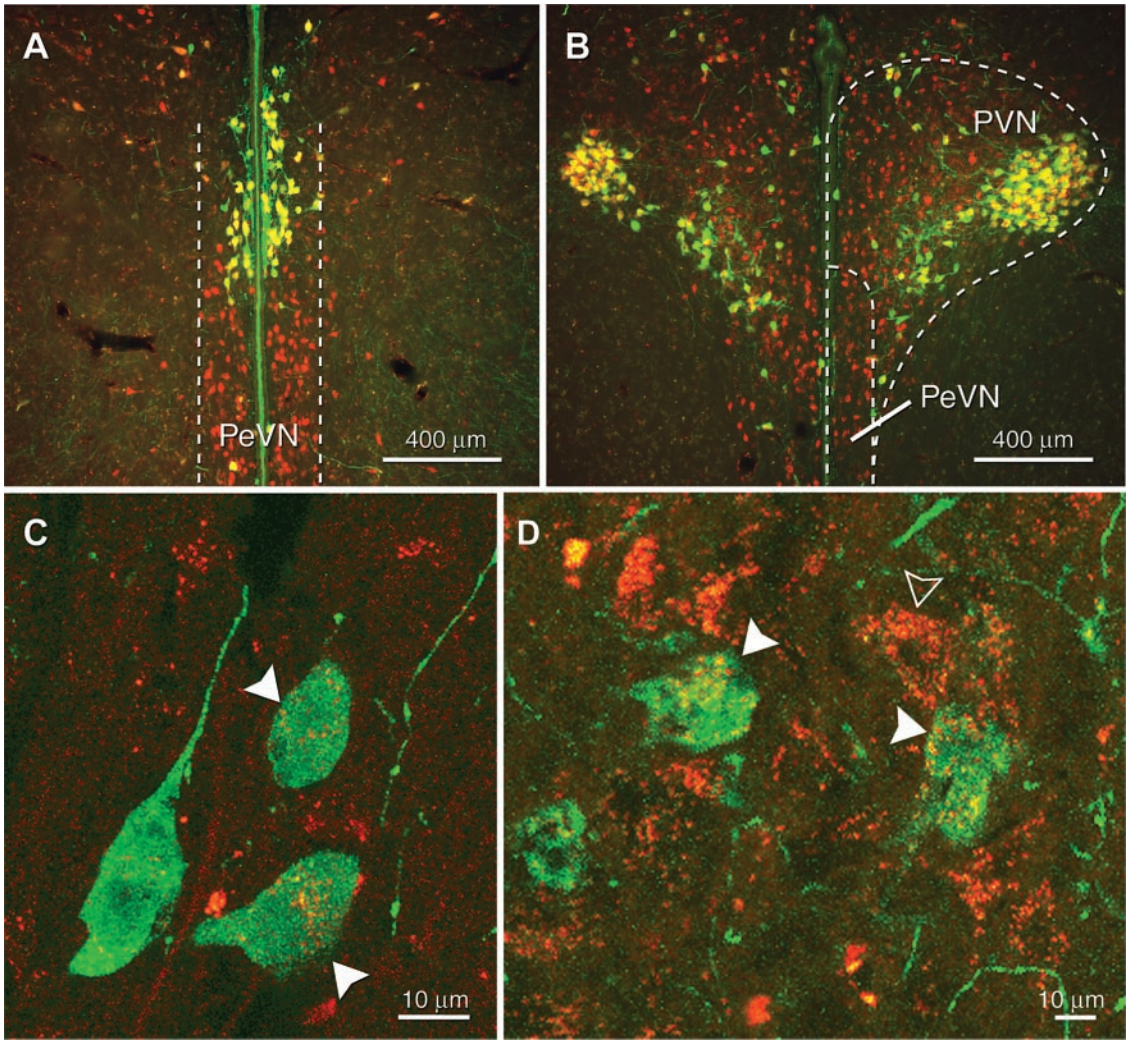

FIG. 2. Examples of fluorescent ICC staining for OT and VIP2R in combination with FG in the PeVN and PVN. Double-labeled cells (*yellow staining*) for OT (*green*) and FG (*red*) appeared on coronal sections of the PeVN (A) and the PVN (B). High-magnified confocal laser scan images of the same brain areas also showed double-labeled cells for OT (*green*) and VIP2R (*red*) in the PeVN (C) and the PVN (D). *Filled arrowheads* indicate colocalization of immunostaining for OT and VIP2R and the *outlined arrowhead* indicates receptor staining on a non-OTergic cell.

calculated for four control animals, three VIP AS-ODN-treated animals, and three RS-ODN-treated animals. The readings revealed a reduction from 202.5 ± 3.1 (mean intensity value ± SEM) for the controls down to 174.2 ± 11.2 in VIP AS-ODN-treated animals (Fig 4C). In contrast, the injection of RS-ODN did not affect VIP synthesis. The mean pixel intensity remained high at 199.9 ± 2.9 (n = 3 animals).

Mathematical model of the proposed PRL secretion mechanism

To help interpret the data from this study, we have developed a mathematical model. This provides the means to illustrate our hypothesis of how the different cell populations interact together to produce the rhythmic PRL secretion shown in Fig. 3.

The model components are illustrated in Fig. 5. Experimental data suggest that VIPergic neurons from the SCN provide rhythmic inhibitory input to DA neurons of the arcuate nucleus (24) and to OT neurons of the PVN/PeVN (Fig. 2, C and D; and Refs. 14 and 15). The DA neurons exert sustained inhibitory input to lactotrophs (2), whereas OT neurons impose stimulatory input (Fig. 1). In addition, there are data suggesting that OT neurons in the PVN receive rhythmic stimulatory input (11), represented as factor x in the model. The pathways illustrated in Fig. 5 are incorporated into the mathematical model, which includes time-dependent equations for PRL, DA, and OT concentrations. The model contains what we postulate to be the main components controlling rhythmic PRL secretion in CS rats. For simplicity, other interactions, such as PRL feedback onto DAergic neurons (38, 39), have not been included in this preliminary model.

Figure 6 shows simulations for CS-OVX animals. The N surge of PRL (0300 h, Fig. 6A) is due to a decrease in the DA tone (Fig. 6B), which is caused by the high nighttime level of VIP (Fig. 6C). This elevated VIP activity inhibits the activity of DA neurons, thus eliminating the inhibitory input to the lactotrophs. The OT neurons play little role in the N PRL

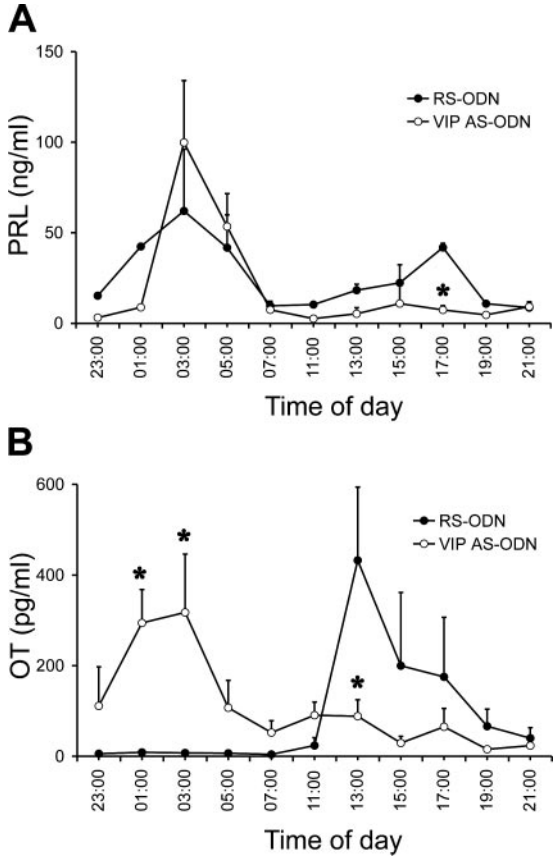

FIG. 3. Effect of PRL (A) and OT (B) secretory patterns in CS-OVX rats after intra-SCN injection of VIP AS-ODN or RS-ODN as control. A, Only nocturnal PRL surges were measured in the serum of VIP AS-ODN-treated animals (*outlined circles*, n = 4) in contrast to the typical nocturnal and diurnal PRL surges in control animals (*filled circles*, n = 5). B, Instead of a prominent afternoon OT surge like in the control animals (*filled circles*, n = 5) there was a nocturnal secretory OT peak coincident with the PRL peak (*outlined circles*, n = 5). Values are expressed as mean ± SEM nanograms per milliliter of PRL, mean ± SEM picograms per milliliter of OT. *, Significant differences compared with RS-ODN ($P < 0.05$).

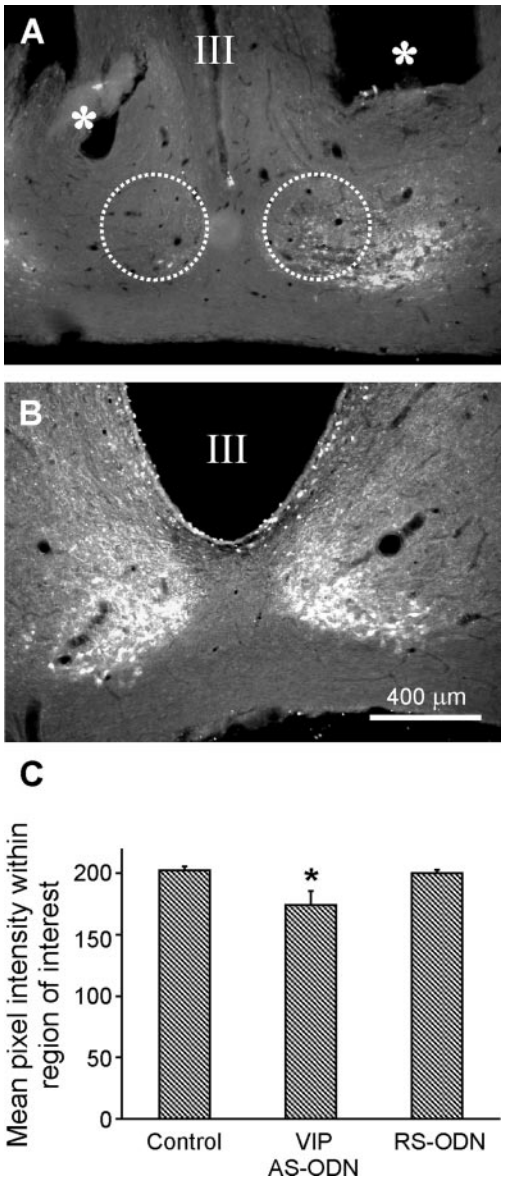

FIG. 4. Reduction of VIP immunoreactivity in the SCN after the bilateral injection of AS-ODN complementary to the rat VIP-mRNA. Representative photomicrographs of VIP immunoreactivity in SCN brain sections of AS-ODN-treated animals (A). In this example, the reduction elicted was particularly striking. *, Former placement of the tip of the bilateral cannulae. B, Representative photomicrograph of VIP immunoreactivitay in SCN brain sections of control animals. C, Bar graph of the mean pixel intensities (*gray values*) within the core region of SCN (d = 400 μm, *dashed circles* in A) of controls (c, n = 4 animals), and VIP AS-ODN (n = 3 animals) as well as RS oligo (RS-ODN, n = 3 animals)-treated rats. Only the VIP AS-ODN treatment caused a significant reduction (*, $P < 0.05$) of the VIP immunoreactivity. Values are expressed as mean gray values ± SEM. III, Third ventricle.

surge because their activity is also inhibited by the elevated VIPergic input (Fig. 6B). In the afternoon, the VIPergic input to DA and OT neurons is greatly reduced (Fig. 6C). As a result, the DA tone is greater in the afternoon, providing inhibitory input to the lactotrophs (Fig. 6B). However, there is an afternoon increase in the activity of OT neurons due to drive from a stimulatory x-factor and no inhibitory VIP input (Fig. 6, B and C). This leads to the D surge of PRL. Because of the higher DA tone at this time of the day, the peak PRL level does not reach the N values (Fig. 6A). The identity of the x-factor is unknown at this time, although there is evidence that serotonin plays this role (8, 11).

Discussion

Data from this study elucidate the role that OT and VIP play in regulating PRL secretion of rats stimulated in the uterine cervix. Factors other than OT and VIP may be more important in controlling estrogen- or suckling-induced PRL surges. It is indeed possible that VIP is but one member of a family of neurotransmitters originating in the SCN that regulates PRL secretion via inhibitor and stimulator factors such as DA and OT, which differ in various physiological states.

Results from the Ca^{2+} imaging experiments in combination with measurements of PRL highlighted the ability of OT to induce PRL secretion from lactotrophs in a dose-dependent manner. These experiments demonstrated simulta-

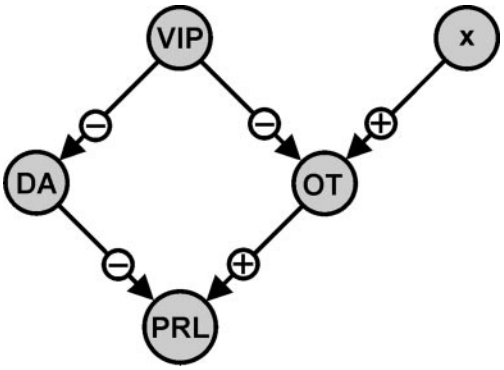

FIG. 5. Outline of the network proposed to be involved in the regulation of the rhythmic PRL secretory pattern in CS rats (N and D surges). VIP of SCN relays time-of-day information to DAergic and OTergic neurosecretory cells via inhibition. An additional stimulatory input (x-factor) is suggested to feed onto OT neurons. DA neurons provide inhibitory input, whereas OT neurons provide stimulatory input to the lactotrophs.

neous elevation of $[Ca^{2+}]_i$ and a PRL surge in response to OT application. Therefore, our findings bridge the results from studies demonstrating the pivotal role of $[Ca^{2+}]_i$ changes in the regulation of PRL secretion from lactotrophs (37) and the secretion of PRL in a dose-dependent fashion during OT treatment of dispersed anterior pituitary cells from lactating rats (40). The biphasic change in the $[Ca^{2+}]_i$ response after OT treatment indicates an initial depletion of intracellular Ca^{2+} stores followed by the opening of Ca^{2+} channels (41, 42). Further experiments need to be done to clarify the mechanism of this biphasic $[Ca^{2+}]_i$ change. The fact that 31% of the cells (lactotroph-enriched cell population) responded to OT with enhanced $[Ca^{2+}]_i$ emphasizes the well-known heterogeneity in the response of lactotrophs to secretagogues (43).

The results from the ICC experiments using OT and VIP2R antibodies in combination with FG suggests that VIP controls neurosecretory OT cells. The neurosecretory nature of OTergic cells in the PeVN and PVN was clearly demonstrated by the colocalization of FG (retrogradely transported neurotracer, iv applied) and OT immunostaining. Neuronal tracing studies have proven that the median eminence receives fibers from parvocellular and magnocellular OT neurons in the PVN (44) and from neurosecretory cells located in the PeVN (45). Therefore, release of OT from these PeVN and PVN neurons may occur in the median eminence. From there, OT could be further transported to the anterior pituitary gland via the long portal vessels. The pituitary portal vascular system has been proposed to be a window for the central OT neurotransmission to pituitary lactotrophs (44, 46). Alternatively, our detection of OT in the peripheral blood could reflect an overflow from magnocellular cells comprising the hypothalamo-hypophyseal tract to the sinusoids in the posterior lobe and thus could be the route through which OT reaches the anterior pituitary or reflect the delivery through the short portal vessels. Because our results do not distinguish between a magnocellular or parvocellular origin of OT reaching the lactotrophs, additional investigations are needed to further clarify which of the different subpopulations of neurosecretory OT cells in the PVN and PeVN are responsible for the OT stimulation of lactotrophs in CS rats.

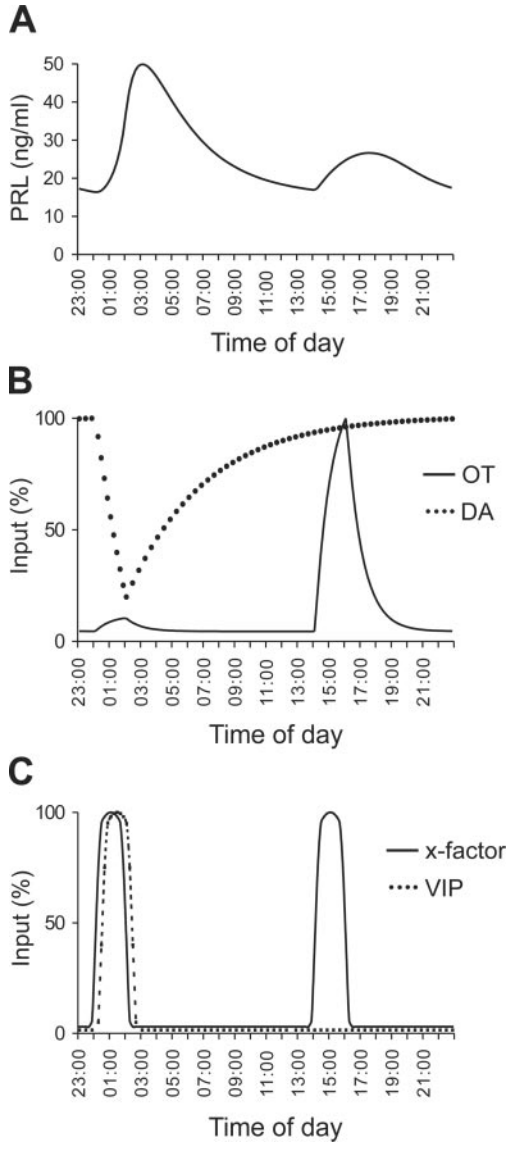

FIG. 6. PRL, OT, and DA secretion patterns for CS-OVX rats simulated by the mathematical model. The amount of secreted PRL (A) depends on the input of stimulatory OT (B) and inhibitory DA (B) at any given time. Timing of surges is controlled by the trigger factors VIP and x-factor, which provide input to OT and DA neurons (C). The first PRL surge is primarily due to reduction in the inhibitory DA tone, whereas the second is mainly due to stimulation from OT neurons. The values for OT, DA, VIP, and the x-factor have been normalized to their peak values.

Because PRL surges in CS rats appear in two narrow time windows every day and seem to be light entrained (47, 48), it is likely that these events are triggered by mechanisms involving the light-sensing SCN. VIP synthesis in the SCN is mainly regulated by lighting conditions, causing daily fluctuation (17–19). Because PIH and PRH regulate PRL secretion from lactotrophs in the anterior pituitary gland, it is presumed that the SCN controls these two offsetting factors to govern the PRL surges. VIP would therefore relay time-of-day information to DA neurons as well as OT neurons. Gerhold *et al.* (24, 26) demonstrated that VIP from the SCN relays time-of-day information to neuroendocrine DAergic neurons

by inhibiting the release of the important PIH DA. Although we did not verify a direct connection of VIPergic neurons from the SCN to neurosecretory OT cells, it is reasonable to assume such a link based on our ICC experiments demonstrating VIP2R immunoreactivity on FG-labeled OT neurons. Furthermore, neuronal connection from SCN to the PVN has also been described using different tract-tracing techniques (14, 15). Buijs *et al.* (49) revealed VIP-containing SCN efferents traveling along the wall of the third ventricle to the PVN. In addition, the authors argued that the rostral PVN, the periventricular PVN and the dorsomedial hypothalamus are excellent candidates for SCN-PVN interactions.

Assuming that VIP controls the activity of DA and OT neurons, an interruption of VIP synthesis in the SCN should consequently alter the PRL release pattern. Indeed, our VIP AS-ODN experiments confirmed such a relationship by demonstrating changes in the timing of PRL and OT surges.

The PRL and OT secretory pattern shown in Fig. 3 can be explained by assuming that VIP exerts an inhibitory influence on OTergic and DAergic neurons. Elevated VIP mRNA and peptide content in the SCN at night could indicate an increased VIPergic signaling to target areas (18), including PVN, PeVN, and arcuate nucleus. Studies in which the VIP content in PVN was determined, revealed a higher content between 2200 h and 0600 h than during the rest of the day (11). However, further experiments are necessary to define the daily release pattern of VIP at the terminals. The enhanced inhibitory input to the DA and OT neurons consequently decrease their activity. As a result, the reduced DA tone would initiate the nocturnal PRL surge. At this time, the activity of the OT neurons would be damped through inhibition by VIP. During the day, there would be less inhibition of the DA and OT neurons due to the low VIP expression in the SCN. An additional trigger signal is needed to induce the release of OT that would initiate the D PRL surge. Serotonin may represent such a trigger (factor x), based on earlier data for its involvement in the regulation of the D PRL surge in CS-OVX rats (8). Because there is less inhibition of DA neurons by VIP in the afternoon, the OT-induced afternoon PRL surge would be smaller than the morning surge (50). To test our hypothesis, further experiments need to be done to clarify the secretory pattern of VIP as well as 5-HT at these OT and DA neurons.

The injection of VIP AS-ODN into the SCN-dampened VIP synthesis (24). According to the notion that VIP exerts an inhibitory influence on DAergic and OTergic neurons, inhibition of both types of neurosecretory cells would be reduced by the AS-ODN treatment. The fact that we could still measure morning OT and PRL surges in these CS rats supports the idea of the existence of a rhythmic VIP-independent x-factor that stimulates OT neurons initiating the PRL surge. In contrast, the lack of the afternoon surges of OT and PRL indicates a VIP dependence of SCN origin. Because there would be no VIP inhibition to OT neurons in the VIP AS-ODN-treated animals in the morning, the stimulatory input to the OT neurons by the x-factor could produce an OT and thus PRL surge. However, the VIP dependence of the afternoon x-factor would make it impossible to generate a stimulatory input in VIP AS-ODN-treated animals. Therefore, we could only measure morning OT and PRL surges.

The results of the ODN experiments suggest that VIP is not the only SCN transmitter signal controlling the PRL surges in CS rats. The remaining question is whether other SCN neurochemicals like arginine vasopressin are directly or indirectly involved in forming the morning x-factor stimulus. This non-VIP-dependent stimulatory input could also account for the remaining PRL surges in CS rats held in constant dark (47). Further experimental studies are required to verify this hypothesis.

Mathematical modeling was used to illustrate our hypothesis of how VIP of SCN origin can serve as a timing signal to control DAergic and OTergic neurosecretory cells, which in turn controls PRL secretion from lactotrophs. In our model, the N PRL surge in CS-OVX animals is due primarily to decreased DA tone, whereas the D PRL surge is due to pronounced OT stimulation. The model simulations demonstrate that the proposed interactions within this small network might be responsible for the regulation of rhythmic PRL secretion in CS-OVX rats.

Whereas the mathematical model illustrates the self-consistency of our hypothesis for rhythmic PRL secretion, it in no way proves that other processes are not involved. Also, model parameters where chosen to illustrate our hypothesis, and were not independently calibrated. Despite these caveats, the model has provided an important prediction, that daily stimulatory input (x-factor) is provided to OT neurons. Clarification of the source of this stimulatory factor is a target of future work.

In summary, our results suggest that OT is a potent PRH that stimulates lactotrophs via Ca^{2+}-dependent mechanisms. Furthermore, neurosecretory OT cells in the PVN and PeVN showed VIP2R expression. The injection of VIP AS-ODN into the SCN caused an alteration in the OT and PRL secretory rhythms of CS-OVX rats, which indicates that VIP of SCN origin could control the activity of neurosecretory OT cells in the PeVN and the PVN. Therefore, light-entrained VIP from the SCN may relay time-of-day information to neurosecretory OT cells in the PeVN and the PVN, triggering PRL secretion from lactotrophs in the anterior pituitary gland.

Acknowledgments

We gratefully acknowledge the technical support of Cheryl Fitch-Pye and Charles Badland as well as the assistance of Kim Riddle and Jon Ekman from the Biological Sciences Imaging Resource at Florida State University. We also thank Dr. Béla Kanyicska (University of Mississippi, Jackson, MS) for critical reading of the manuscript and Dr. Albert Parlow (National Hormone and Pituitary Program, Torrance, CA) for RIA reagents.

Received December 17, 2003. Accepted March 10, 2004.

Address all correspondence and requests for reprints to: Marc E. Freeman, Biomedical Research Facility, Florida State University, Tallahassee, Florida 32306-4340. E-mail: freeman@neuro.fsu.edu.

This work was supported by a fellowship of the Lalor Foundation (to M.E.), National Science Foundation Grant DMS 0311856 (to R.B.), and National Institutes of Health Grant DK43200 (to M.F.).

References

1. **Freeman ME, Kanyicska B, Lerant A, Nagy G** 2000 Prolactin: structure, function, and regulation of secretion. Physiol Rev 80:1524–1631
2. **Ben-Jonathan N** 1985 Dopamine: a prolactin-inhibiting hormone. Endocr Rev 6:564–589

3. **Ben-Jonathan N, Hnasko R** 2001 Dopamine as a prolactin (PRL) inhibitor. Endocr Rev 22:724–763
4. **DeGreef WJ, Neill JD** 1979 Dopamine levels in hypophysial stalk plasma of the rat during surges of prolactin secretion induced by cervical stimulation. Endocrinology 105:1093–1099
5. **McKay DW, Pasieka CA, Moore KE, Riegle GD, Demarest KT** 1982 Semicircadian rhythm of tuberoinfundibular dopamine neuronal activity during early pregnancy and pseudopregnancy in the rat. Neuroendocrinology 34: 229–235
6. **Erskine MS** 1995 Prolactin release after mating and genitosensory stimulation in females. Endocr Rev 16:508–528
7. **Samson WK, Schell DA** 1995 Oxytocin and the anterior pituitary gland. Adv Exp Med Biol 395:355–364
8. **Arey BJ, Freeman ME** 1990 Oxytocin, vasoactive-intestinal peptide, and serotonin regulate the mating-induced surges of prolactin secretion in the rat. Endocrinology 126:279–284
9. **Breton C, Pechoux C, Morel G, Zingg HH** 1995 Oxytocin receptor messenger ribonucleic acid: characterization, regulation, and cellular localization in the rat pituitary gland. Endocrinology 136:2928–2936
10. **Gainer H, Wray S** 1994 Cellular and molecular biology of oxytocin and vasopressin. In: Knobil E, Neill JD, eds. The physiology of reproduction. New York: Raven Press; 1099–1129
11. **Arey BJ, Freeman ME** 1992 Activity of oxytocinergic neurons in the paraventricular nucleus mirrors the periodicity of the endogenous stimulatory rhythm regulating prolactin secretion. Endocrinology 130:126–132
12. **Weaver DR** 1998 The suprachiasmatic nucleus: a 25-year retrospective. J Biol Rhythms 13:100–112
13. **Moore RY, Speh JC, Leak RK** 2002 Suprachiasmatic nucleus organization. Cell Tissue Res 309:89–98
14. **Watts AG, Swanson LW, Sanchez-Watts G** 1987 Efferent projections of the suprachiasmatic nucleus: I. Studies using anterograde transport of *Phaseolus vulgaris* leucoagglutinin in the rat. J Comp Neurol 258:204–229
15. **Teclemariam-Mesbah R, Kalsbeek A, Pevet P, Buijs RM** 1997 Direct vasoactive intestinal polypeptide-containing projection from the suprachiasmatic nucleus to spinal projecting hypothalamic paraventricular neurons. Brain Res 748:71–76
16. **Sheward WJ, Lutz EM, Harmar AJ** 1995 The distribution of vasoactive intestinal peptide2 receptor messenger RNA in the rat brain and pituitary gland as assessed by in situ hybridization. Neuroscience 67:409–418
17. **Morin A, Denoroy L, Jouvet M** 1991 Daily variations in concentration of vasoactive intestinal polypeptide immunoreactivity in discrete brain areas of the rat. Brain Res 538:136–140
18. **Okamoto S, Okamura H, Miyake M, Takahashi Y, Takagi S, Akagi Y, Fukui K, Okamoto H, Ibata Y** 1991 A diurnal variation of vasoactive intestinal peptide (VIP) mRNA under a daily light-dark cycle in the rat suprachiasmatic nucleus. Histochemistry 95:525–528
19. **Shinohara K, Tominaga K, Isobe Y, Inouye ST** 1993 Photic regulation of peptides located in the ventrolateral subdivision of the suprachiasmatic nucleus of the rat: daily variations of vasoactive intestinal polypeptide, gastrin-releasing peptide, and neuropeptide Y. J Neurosci 13:793–800
20. **Laemle LK** 1992 Unilateral enucleation alters vasoactive intestinal polypeptide-like immunoreactivity in the suprachiasmatic nucleus of the rat. Brain Res 572:325–328
21. **Gorospe WC, Freeman ME** 1981 The effects of various methods of cervical stimulation on continuation of prolactin surges in rats. Proc Soc Exp Biol Med 167:78–82
22. **Paxinos G, Watson C** 1998 The rat brain in stereotaxic coordinates. 4th ed. London: Academic
23. **Freeman ME, Sterman JR** 1978 Ovarian steroid modulation of prolactin surges in cervically stimulated ovariectomized rats. Endocrinology 102:1915–1920
24. **Gerhold LM, Sellix MT, Freeman ME** 2002 Antagonism of vasoactive intestinal peptide mRNA in the suprachiasmatic nucleus disrupts the rhythm of FRAs expression in neuroendocrine dopaminergic neurons. J Comp Neurol 450:135–143
25. **Watson Jr RE, Wiegand SJ, Clough RW, Hoffman GE** 1986 Use of cryoprotectant to maintain long-term peptide immunoreactivity and tissue morphology. Peptides 7:155–159
26. **Gerhold LM, Horvath TL, Freeman ME** 2001 Vasoactive intestinal peptide fibers innervate neuroendocrine dopaminergic neurons. Brain Res 919:48–56
27. **Turgeon JL, Shyamala G, Waring DW** 2001 PR localization and anterior pituitary cell populations in vitro in ovariectomized wild-type and PR-knockout mice. Endocrinology 142:4479–4485
28. **Dalcík H, Phelps CJ** 1993 Median eminence-afferent vasoactive intestinal peptide (VIP) neurons in the hypothalamus: localization by simultaneous tract tracing and immunocytochemistry. Peptides 14:1059–1566
29. **Horvath TL** 1997 Suprachiasmatic efferents avoid phenestrated capillaries but innervate neuroendocrine cells, including those producing dopamine. Endocrinology 138:1312–1320
30. **Luther JA, Daftary SS, Boudaba C, Gould GC, Halmos KC, Tasker JG** 2002 Neurosecretory and non-neurosecretory parvocellular neurones of the hypothalamic paraventricular nucleus express distinct electrophysiological properties. J Neuroendocrinol 14:929–932
31. **Livingstone JD, Lerant A, Freeman ME** 1998 Ovarian steroids modulate responsiveness to dopamine and expression of G-proteins in lactotropes. Neuroendocrinology 68:172–179
32. **Velkeniers B, Hooghe-Peters EL, Hooghe R, Belayew A, Smets G, Claeys A, Robberecht P, Vanhaelst L** 1988 Prolactin cell subpopulations separated on discontinuous Percoll gradient: an immunocytochemical, biochemical, and physiological characterization. Endocrinology 123:1619–1630
33. **Gershengorn MC, Osman R** 1996 Molecular and cellular biology of thyrotropin-releasing hormone receptors. Physiol Rev 76:175–191
34. **Ashworth R, Hinkle PM** 1996 Thyrotropin-releasing hormone-induced intracellular calcium responses in individual rat lactotrophs and thyrotrophs. Endocrinology 137:5205–5212
35. **Burris TP, Freeman ME** 1993 Low concentrations of dopamine increase cytosolic calcium in lactotrophs. Endocrinology 133:63–68
36. **Ermentrout B** 2002 Simulating, analyzing and animating dynamical systems: a guide to XPPAUT for researchers and students. Philadelphia: Society for Industrial and Applied Mathematics
37. **Huang CY, Kuo WW, Tsai TP, Wu DJ, Hsieh YS, Wang PS, Cheng CK, Liu JY** 2002 Prolactin secretion and intracellular Ca(2+) change in rat lactotroph subpopulations stimulated by thyrotropin-releasing hormone. J Cell Biochem 87:126–132
38. **DeMaria JE, Nagy GM, Freeman ME** 2000 Immunoneutralization of prolactin prevents stimulatory feedback of prolactin on hypothalamic neuroendocrine dopaminergic neurons. Endocrine 12:333–337
39. **Lerant AA, DeMaria JE, Freeman ME** 2001 Decreased expression of fos-related antigens (FRAs) in the hypothalamic dopaminergic neurons after immunoneutralization of endogenous prolactin. Endocrine 16:181–187
40. **Samson WK, Lumpkin MD, McCann SM** 1986 Evidence for a physiological role for oxytocin in the control of prolactin secretion. Endocrinology 119:554–550
41. **Carew MA, Mason WT** 1995 Control of Ca2+ entry into rat lactotrophs by thyrotrophin-releasing hormone. J Physiol 486:349–360
42. **Fomina AF, Levitan ES** 1995 Three phases of TRH-induced facilitation of exocytosis by single lactotrophs. J Neurosci 15:4982–4991
43. **Castaño JP, Kineman RD, Frawley LS** 1996 Dynamic monitoring and quantification of gene expression in single, living cells: a molecular basis for secretory cell heterogeneity. Mol Endocrinol 10:599–605
44. **Zimmerman EA, Nilaver G, Hou-Yu A, Silverman AJ** 1984 Vasopressinergic and oxytocinergic pathways in the central nervous system. Fed Proc 43:91–96
45. **Swanson LW, Sawchenko PE** 1983 Hypothalamic integration: organization of the paraventricular and supraoptic nuclei. Annu Rev Neurosci 6:269–324
46. **Sarkar DK, Gibbs DM** 1984 Cyclic variation of oxytocin in the blood of pituitary portal vessels of rats. Neuroendocrinology 39:481–483
47. **Bethea CL, Neill JD** 1979 Prolactin secretion after cervical stimulation of rats maintained in constant dark or constant light. Endocrinology 104:870–876
48. **Yogev L, Terkel J** 1980 Effects of photoperiod, absence of photic cues, and suprachiasmatic nucleus lesions on nocturnal prolactin surges in pregnant and pseudopregnant rats. Neroendocrinology 31:26–33
49. **Buijs RM, Markman M, Nunes-Cardoso B, Hou YX, Shinn S** 1993 Projections of the suprachiasmatic nucleus to stress-related areas in the rat hypothalamus: a light and electron microscopic study. J Comp Neurol 335:42–54
50. **Smith MS, Freeman ME, Neill JD** 1975 The control of progesterone secretion during the estrous cycle and early pseudopregnancy in the rat: prolactin, gonadotropin and steroid levels associated with rescue of the corpus luteum of pseudopregnancy. Endocrinology 96:219–226

***Endocrinology* is published monthly by The Endocrine Society (http://www.endo-society.org), the foremost professional society serving the endocrine community.**